

Insolation forcing of Holocene climate change in Southern California: a sediment study from Lake Elsinore

Matthew E. Kirby · Steve P. Lund · Michael A. Anderson ·
Broxton W. Bird

Received: 27 February 2006 / Accepted: 11 December 2006 / Published online: 25 January 2007
© Springer Science+Business Media B.V. 2007

Abstract Lake Elsinore is the largest natural lake in Southern California. As such, the lake provides a unique opportunity to investigate terrestrial climate on timescales otherwise under-represented in the region's terrestrial environment. In November 2003, three ~10 m drill cores were extracted from the depocenter region of Lake Elsinore. These drill cores, spanning the past 9,500–11,200 calendar years, represent the first complete Holocene record of terrestrial climate from Southern California. In this paper, we focus on two adjacent, depocenter cores (LEGC03-2

and LEGC03-3), which have been correlated to develop a single composite core. Twenty-two AMS ^{14}C dates on bulk organic matter and one cross-correlated exotic pollen age constitute the composite core's age control. Several methods of analysis, including mass magnetic susceptibility, % total organic matter, % total carbonate, % HCl-extractable Al, and total inorganic P are used to infer climate for the past 9,500 calendar years in Southern California. Together, these data indicate a wet early Holocene followed by a long-term drying trend. Recent lake-level reconstructions from Owens Lake and Tulare Lake support our contention for a wetter-than-today early Holocene. Lacustrine sediments from the Mojave Desert also support our conclusions. We suggest that over the duration of the Holocene changing summer/winter insolation alters the region's long-term hydrologic balance through its modulation of atmospheric circulation and its associated storm tracks. Minimum early Holocene winter insolation and maximum summer insolation act together to increase the region's total annual precipitation by increasing the frequency of winter storms as well as enhancing the magnitude and spatial extent of the North American monsoon, the frequency of land-falling tropical cyclones in Southern California, and regional convective storms, respectively. Gradual decreases in summer insolation and increases in winter insolation produce the opposite effect with maximum drying in the late Holocene.

M. E. Kirby (✉) · B. W. Bird
Department of Geological Sciences,
California State University, Fullerton,
Fullerton, CA 92834, USA
e-mail: mkirby@fullerton.edu

S. P. Lund
Department of Earth Sciences,
University of Southern California, Los Angeles,
CA 90089, USA
e-mail: slund@usc.edu

M. A. Anderson
Department of Environmental Sciences,
University of California, Riverside, Riverside,
CA 92521, USA
e-mail: michael.anderson@ucr.edu

B. W. Bird
Department of Earth Sciences,
University of Pittsburgh, Pittsburgh, PA, USA
e-mail: bwb8@pitt.edu

Keywords Holocene · Lake Elsinore · Sediments · Insolation

Introduction

Southern California is highly sensitive to climate variability (Inman and Jenkins 1999; Wilkinson et al. 2002; Beuhler 2003; Miller and Strem 2003). Predictions of future climate change in a global warming world indicate that larger-than-present amplitude variability will characterize the climate system (IPCC 2001). This shift in the dominant scale of climate variability includes more severe floods and droughts (IPCC 2001; Beuhler 2003). To properly assess present and future climate variability in Southern California, the reconstruction and interpretation of a baseline of past climate variability under different climate states and forcings is essential. It should be noted that in this paper, the term Southern California is used to represent the highly populated coastal region south of Santa Barbara to the Mexican border and east, including the Transverse and Peninsular Ranges.

Historical records of climate variability in Southern California have been maintained for less than 150 years, too short a period to provide a robust understanding of the forcing mechanisms and dynamics of multi-scale (e.g. multi-decadal-to-centennial scale) climate variability. This interval is also too short to provide a robust, frequency distribution analysis of extreme climate-related events, such as large storms and severe droughts. In turn, the prehistoric record (>150 years) of climate variability in Southern California is sparsely documented, and limited to Mission diaries, tree-ring studies, some palynology, and low-resolution lake studies (Lynch 1931; Heusser 1978; Meko and Boggess 1980; Rowntree 1985; Davis 1992; Enzel et al. 1992; Filippelli and Souch 1999; Cole and Wahl 2000; Filippelli et al. 2000; Biondi et al. 2001; D'Arrigo et al. 2001; Byrne et al. 2003; Kirby et al. 2004, 2005, 2006; Gervais 2006; Bird and Kirby 2006).

The high-resolution marine records from Santa Barbara Basin (SBB) are the most complete Holocene records for the region (e.g. Heusser 1978; Pisias 1978; Friddell et al. 2003; Kennett

2005). It remains unclear, however, how the ocean's response to climate change transfers to the terrestrial realm. For example, how does a 2°C change in sea surface temperature off the coast the Southern California relate to the region's terrestrial climate? This dearth of complete, high-resolution, terrestrial, Holocene records from Southern California has limited scientists' ability to evaluate and compare existing records of Holocene climate variability in western North America (e.g. Tulare Lake, Owens Lake, and Pyramid Lake) to Southern California. Consequently, there are many unresolved questions concerning the causal mechanisms driving Holocene climate in western North America and how climate is manifest in terms of development, variability, and spatial-temporal patterns.

In Southern California there is a relatively untapped resource for documenting both historical and pre-historical/geological patterns of climate variability—lakes (Davis 1992; Filippelli and Souch 1999; Cole and Wahl 2000; Filippelli et al. 2000; Kirby et al. 2004, 2005, 2006; Bird and Kirby 2006). Lakes have the capacity to record climate information over a wide range of spatial and temporal scales; therefore, lakes provide an excellent archive for documenting multi-scale climate variability (e.g. Kelts and Talbot 1990; Drummond et al. 1995; Benson et al. 1996; Anderson et al. 1997; Teranes and McKenzie 2001; Kirby et al. 2002a, b; Rosenmeier et al. 2002).

As part of an on-going investigation of past climate variability in Southern California, there are several lakes under study from a variety of environments (i.e. elevations, sizes, drainage basins). For this part of the research project, we focus on Lake Elsinore, a natural lake located 120 km southeast of downtown Los Angeles and present results from two recently acquired drill cores from the lake's depocenter (Figs. 1, 2). This paper's objectives are threefold: (1) to present the initial drill core results from Lake Elsinore in the context of the composite core and its chronology; (2) to present the initial sedimentological analyses including mass magnetic susceptibility, % total organic matter, % total carbonate, % HCl-extractable Al, and total inorganic phosphorus; and, (3) to interpret these data in the context of orbital-scale Holocene climate change.

Fig. 1 Regional map view of study site. NA = North America; PO = Pacific Ocean; LE = Lake Elsinore; CA = California; NV = Nevada; OL = Owens Lake; TL = Tulare Lake; SL = Silver Lake; SJM = San Joaquin Marsh; Dashed line with arrows show location of TR = Transverse Range and PR = Peninsular Range, which delimit the boundaries of Southern California as discussed in the text

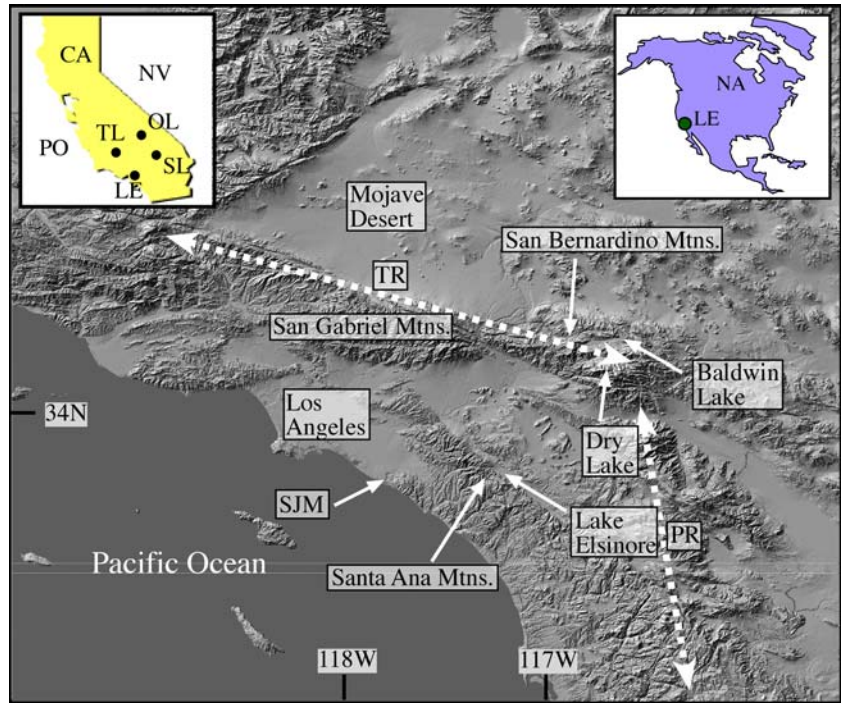
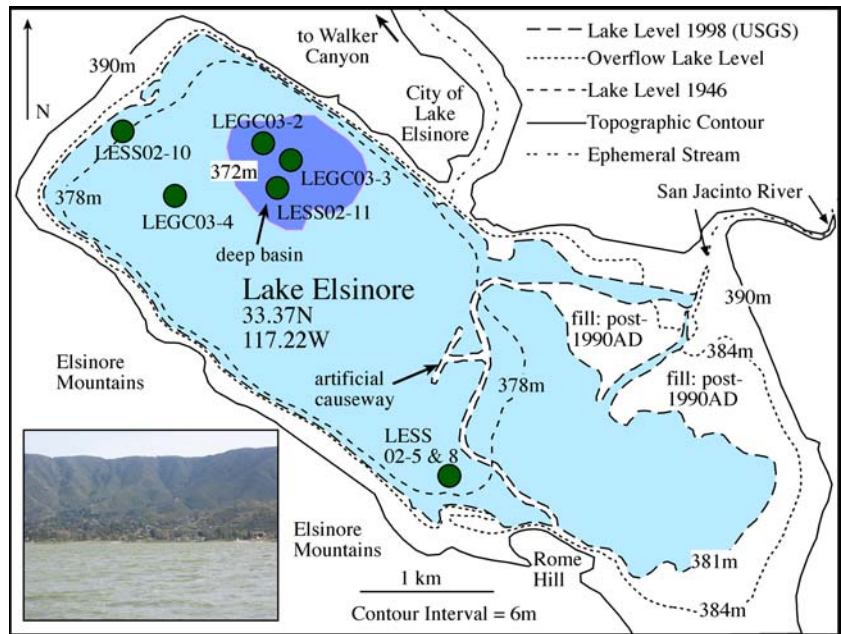


Fig. 2 Study site map with relevant cores. Deep basin floor was 5 m below 2003 surface of ~376 m above sea level. Cores LESS02-5, 8, and 10 are the littoral cores discussed in Kirby et al. (2004, 2005). Inset photo shows Elsinore Mountains looking southwest from the lake center



Background

Relationship between Lake Elsinore and regional climate

Precipitation variability in present-day Southern California is dominated by the winter season (defined here as December–February) (Lynch 1931; Redmond and Koch 1991). In Southern California, the amount of precipitation is related to the average position of the winter season polar front, which responds to changes in the position of the eastern Pacific subtropical high. Historically, dry winters in Southern California are associated with a strong high-pressure ridge off the western coast of the United States, which steers storms over the northwestern United States. Wet winters are linked to a weakening of the subtropical high, causing the storm track to shift southward (Pyke 1972; Cayan and Roads 1984; Lau 1988; Schonher and Nicholson 1989; Redmond and Koch 1991). In turn, the large-scale atmospheric patterns that control the average position of the polar front are modulated by Pacific Ocean sea-surface conditions (Namias and Cayan 1981; Douglas et al. 1983; Latif and Barnett 1994; Trenberth and Hurrell 1994; Cayan et al. 1998; Dettinger et al. 1998). Interannual precipitation variability over Southern California is also linked with El Niño–Southern Oscillation (ENSO hereafter; El Niño = higher ppt. in Southern CA and vice versa in northern CA) and interdecadal precipitation variability to the Pacific Decadal Oscillation (PDO hereafter; +PDO similar to El Niño effects) (e.g. Schonher and Nicholson 1989; Redmond and Koch 1991; Biondi et al. 2001; Mantua and Hare 2002).

Kirby et al. (2004) examined the relationship between historic lake levels at Lake Elsinore and regional winter precipitation. The analysis indicates a strong positive correlation between total winter precipitation for Los Angeles/San Diego/Lake Elsinore and Lake Elsinore lake level for the historic record (Fig. 3). A comparison between PDO and lake-level also shows a positive relationship, which indicates that large-scale ocean–atmosphere interactions are recorded at our study site (Fig. 3). Together, these analyses suggest that Lake Elsinore

responds to a broad range of spatial and temporal hydrologic forcings.

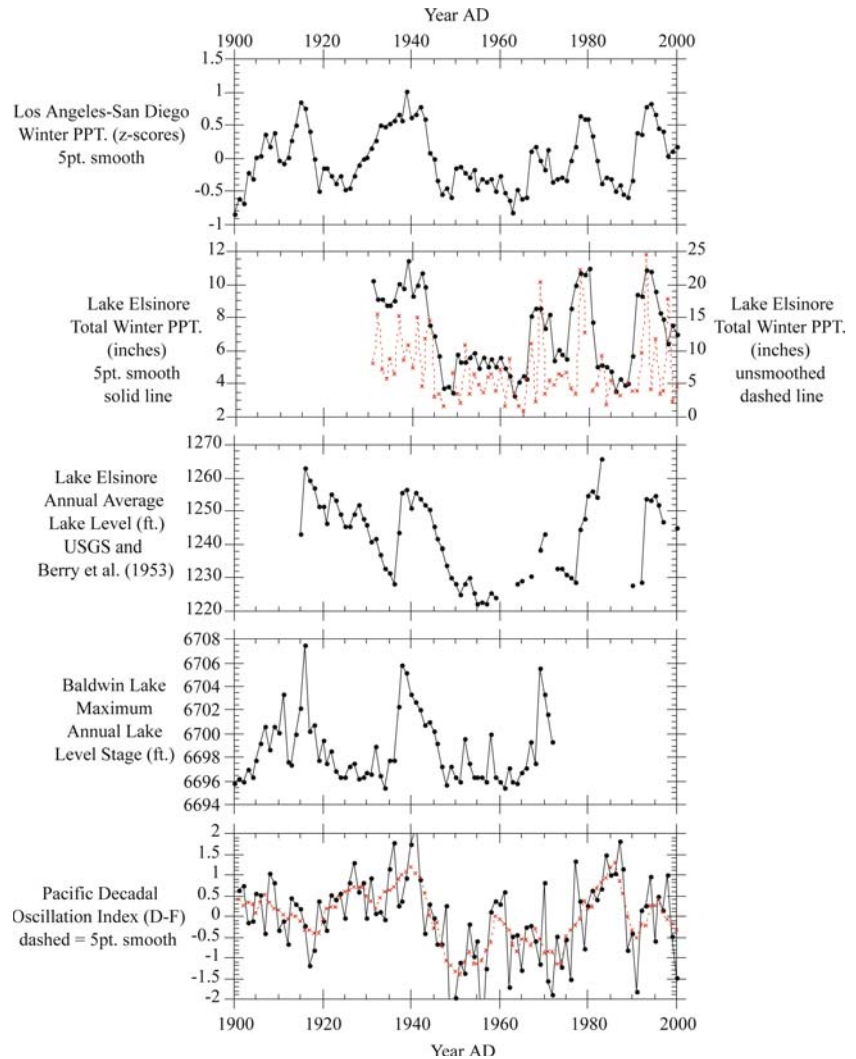
Under present conditions, the contribution of summer–fall precipitation to Southern California is considered small (Tubbs 1972; Tang and Reiter 1984; Douglas et al. 1993; Adams and Comrie 1997). Although summer precipitation is rare, the effects can be severe, resulting in floods, landslides, and lightning produced forest fires (Tubbs 1972). Generally, summer precipitation is produced by either an expansion of the North American monsoon, which enhances local atmospheric convection and its associated thunderstorms, or waning tropical cyclones (Tubbs 1972). In fact, there have been 39 years with measurable precipitation attributed to waning tropical cyclones in Southern California between 1900 and 1997 AD (Williams 2005).

Lake Elsinore as a study site

Lake Elsinore, located 120 km SE of Los Angeles, California, is the largest of only a few natural, permanent lakes in Southern California (Figs. 1, 2). Known to the Pai-ah-che Indians as Etengvo Wumoma—or Hot Springs by the Little Sea—Lake Elsinore has long been a site of human occupation (Hudson 1978). In fact, Grenda (1997) found evidence for continuous human activity along the shores of Lake Elsinore for the entire time frame studied—8,400 years.

Lake Elsinore is a structural depression formed within a graben along the Elsinore fault (Mann 1956; Hull 1990). Geologically, Lake Elsinore is surrounded by a combination of predominantly igneous and metamorphic rocks (Engel 1959; Hull 1990). Lake Elsinore is constrained along its southern edge by the steep, deeply incised Elsinore Mountains that rise to more than 1,000 m. The Elsinore Mountains likely provide a local sediment source particularly during extreme precipitation events (Fig. 2; Kirby et al. 2004). Two exploratory wells have been drilled at the east end of the lake to 542 and 549 m, respectively, with sediment described as mostly fine-grained (Anonymous 1979; Damiata and Lee 1986). Gravimetric studies indicate that the Elsinore trough may extend to greater than 900 m depth (Hull 1990).

Fig. 3 Regional precipitation data, lake level data from Lake Elsinore and Baldwin Lake (French and Busby 1974), and Pacific Decadal Oscillation index values (dashed line = 5pt. smooth; Mantua and Hare 2002)



Lake Elsinore has a relatively small drainage basin (<1,240 km²) from which the San Jacinto River flows (semi-annually) into and terminates within the lake’s basin (Fig. 2) (USGS 1998; Kirby et al. 2004). Lake Elsinore has overflowed to the northwest through Walker Canyon very rarely, only three times in the 20th century and 20 times since 1769 AD based on Mission Diaries (Lynch 1931; USGS Lake level Data). Each overflow event lasted less than several weeks demonstrating that Lake Elsinore is essentially a closed-basin lake system (Lynch 1931; USGS Lake level Data). Conversely, Lake Elsinore has dried completely on only four occasions since 1769 AD (Lynch 1931; USGS Lake level Data).

During this period of historical observation, the deepest parts of the lake remain wet mud while the remaining areas desiccated (Hudson 1978; Lake Elsinore Historical Society per. com. and pictorial archives). Consistent with the historical observations, cores extracted from the deepest part of the profundal zone show no evidence for sediment hiatuses during the documented twentieth century low stands (Kirby et al. 2004). Sedimentologically, lake desiccation events may be characterized by periods of slow or no deposition, but limited, if any, sediment removal within the deepest basin.

Limnologically, Lake Elsinore is a shallow, polymictic lake (13 m maximum depth based on

historic records) (Anderson 2001). A recent study by Anderson (2001) indicates that the hypolimnion is subject to short periods (i.e. days to weeks) of anoxia. Frequent mixing of oxygen rich epilimnion waters into the hypolimnion precludes permanent, sustained anoxia, at least during the period of observation. Water loss to evaporation is >1.4 m/year; consequently, water residence time in Lake Elsinore is projected to be short at all times and shorter during drought periods (Mann 1947; USGS 1998; Anderson 2001). Sediment trap studies also indicate that CaCO₃ is produced within the water column, likely linked to photosynthetic uptake of CO₂ by phytoplankton (Anderson 2001). SEM analyses of lake sediment show distinct micron sized CaCO₃ grains dispersed throughout the sediment (Anderson 2001).

Methods

Sediment analyses

Three sediment cores (LEGC03-2 [949 cm], LEGC03-3 [1074 cm], and LEGC03-4 [994 cm]) were recovered using a barge-mounted, split-spoon corer operated by Gregg Drilling Company (Fig. 2; Table 1). Core LEG03-2, composed of 13 sequential segments (Fig. 1), recovered sediments to a depth of 949 cm below lake bottom with 76% recovery; core LEG03-3, composed of 15 sequential segments (Fig. 1), recovered sediments to a depth of 1,074 cm with 85% recovery. Core LEG03-4 is not discussed in this paper. Cores LEGC03-2 and LEGC03-3 were taken from within 200 m horizontal distance from one another in the lake's present day deepest basin (Fig. 2). Our assumption regarding sediment gaps is that all core drives using the hollow-stemmed auger drill core were to the measured depth. Any

“missing” core sections were subtracted from the top of core's individual drive and assumed a product of over-auguring between drives. Similarly, any “re-worked” sediment at the core top was assumed a product of drilling and was not used for sediment analysis. Lastly, each segment was split in the laboratory, digitally photographed, and archived in cold storage at the Cal-State Fullerton Paleoclimatology Laboratory.

For mass magnetic susceptibility, samples were extracted from LEG03-2 and -3 at 1.0 cm intervals ($n = 1,693$). The samples were placed in pre-weighed 8 cm³ plastic cubes. Mass magnetic susceptibility was measured twice on each sample with the y-axis rotated 180° once per analysis. All samples were analyzed using a Bartington MS2 Magnetic Susceptibility instrument at 0.465 kHz. Measurements were made to the 0.1 decimal place and reported as mass magnetic susceptibility in SI units ($\times 10^{-7}$ m³ kg⁻¹).

Total organic matter (%TOM) and total carbonate (%TC) were determined by loss-on-ignition at 550 and 950°C for 2 h each, respectively (Dean 1974; Heiri et al. 2001). Samples were extracted from cores LEGC03-2 and LEGC03-3 at 1.0 cm intervals ($n = 1,693$). As shown by Dean (1974), three to four percent total weight loss after 950°C may be a function of clay de-watering. Consequently, we interpret values less than three to four percent as essentially zero percent total carbonate.

Percent HCl-extractable Al (%Al) and total inorganic phosphorous (IP) were measured on samples from core LEGC03-3 at 10 cm intervals, except for depths of 0.7–1.4 m, where sediment was collected at 3 cm intervals. Total inorganic P was extracted from separate (unashed) samples of known dry-weight with 1 M HCl for 24 h (Aspila et al. 1976). Dissolved P in the extracts was quantified on an Alpkem autoanalyzer. 1 M HCl-extractable Al was also measured on the IP extracts using a Perkin-Elmer Optima 3000 DV ICP-OES.

Composite core

Cores LEG03-2 and LEG03-3 were correlated to create a composite core in the following a similar procedure as that used by the Ocean

Table 1 Core information (water depth as of November 2003)

Core ID	Water depth (m)	Latitude	Longitude	Core length (cm)
LEGC03-2	5.0	N33°40.330	W117°21.186	949
LEGC03-3	4.9	N33°40.395	W117°21.250	1,074
LEGC03-4	4.0	N33°40.044	W117°21.848	994

Drilling Program (e.g. McGuire and Acton 2003). First, eight distinctive and correlative stratigraphic horizons from the two cores were identified based on inspection of the digital color photographs. Next, a plot was made of each core segment at the same stratigraphic scale to compare the digital color photograph, mass magnetic susceptibility, total organic matter, and total carbonate. Using these plots and the eight distinctive correlative horizons as starting points, the two cores were separately correlated in detail using the core segment plots. Core LEG03-3 was used as the master core because it is longer and contains a higher recovery percentage. Core LEG03-2 was correlated to core LEG03-3 by noting LEG03-2 depths and equivalent LEG03-3 depths. Finally, the individual correlations were compared and minor discrepancies resolved. In most cases, the majority of variability in one core segment could be correlated to a single core segment from the replicate core. The initial correlations for each core segment generally were not pushed to the very upper and lower edges of the segment because of concern that coring artifacts might bias the segment-boundaries data.

Age control

In the absence of salvageable macro- or micro-organic matter, bulk organic matter was used for AMS ^{14}C dating. Samples were pre-treated with an acid wash to remove carbonate. Eight dates were obtained on core LEGC03-2 and 18 dates were obtained on core LEGC03-3. All dates were measured at the University of California, Irvine Keck AMS Facility. The age model for the past 200 years is based on a combination of exotic pollen stratigraphy, ^{137}Cs , and elemental lead (Kirby et al. 2004).

Results

Core descriptions

Sediment descriptions are based on visual estimates of sand, silt, and clay (Fig. 4). Color changes and other notable sedimentological

features are also noted. Core descriptions show the depth of dating analyses. Both cores are characterized by dominantly clay sediments. The cores contain infrequent, but visible CaCO_3 nodules between 750 cm and the core bottom. Thin (<2 cm) silt horizons are present in the lower half of both cores. Core LEGC03-2 contains dispersed faint laminae between 700 cm and 250 cm. A distinct color change occurs in core LEGC03-2 and LEGC03-3 between 695 cm and 690 cm and 715 cm and 610 cm, respectively. In core LEGC03-3, rounded mud clasts(?) occur at 670 cm. Both cores are also characterized by sediment with secondary features such as mud cracks(?) and distinct bioturbation(?) in the upper 350 cm of core LEGC03-2 and the upper 250 cm of core LEGC03-3.

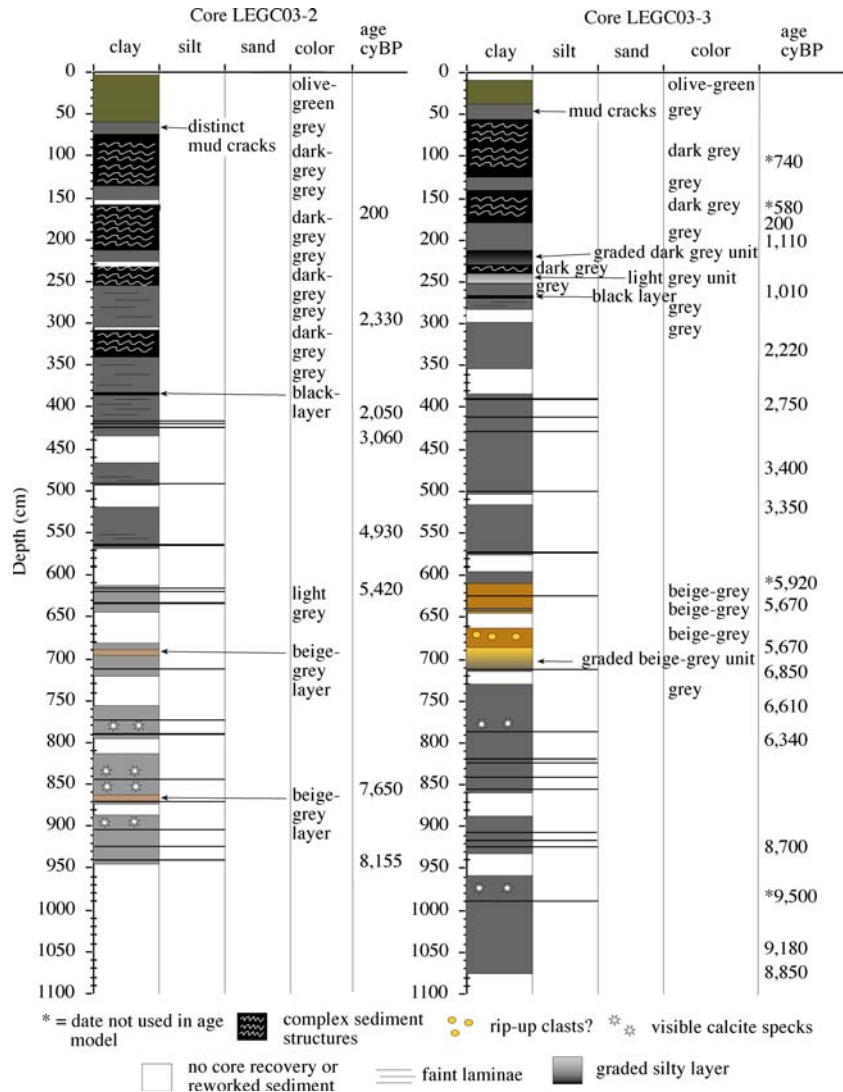
Mass magnetic susceptibility, total organic matter, and total carbonate

Mass magnetic susceptibility values per depth for cores LEGC03-2 and -3 show very similar decreasing trends from the core bottom to the core top (Figs. 5, 6). The highest and most variable values are near the core bottom for both cores. Both cores also show occasional spikes in magnetic susceptibility, some of which are associated with silt-rich layers.

Total organic matter for both cores LEGC03-2 and LEGC03-3 show similar weak increasing trends from the core bottom to the core top (Figs. 5, 6). In addition to this trend, there is also an abrupt increase in the average %TOM values at 400 and 350 cm in cores LEGC03-2 and LEGC03-3, respectively. This abrupt increase in %TOM is also characterized by an increase in the amplitude of variability. Core LEGC 03-3 also shows evidence for an abrupt increase in %TOM at 850 cm. This change is not seen in core LEGC03-2 due to its shorter total length. We also note that there is a strong, positive logarithmic relationship between magnetic susceptibility and %TOM for both cores (Fig. 7).

Total carbonate for both cores LEGC03-2 and LEGC03-3 show similar increasing trends from the core bottom to the core top (Figs. 5, 6). In addition to this trend, there is also an abrupt

Fig. 4 Core LEGC03-2 and LEGC03-3 sediment descriptions with AMS ^{14}C dates converted to calendar years before present



increase in the average values and the amplitude of variability at 530 and 570 cm in cores LEGC03-2 and LEGC03-3, respectively. We note, however, that the several sections of missing data (i.e. sediment) in core LEGC03-2 preclude the absolute depth identification of this increase. There is a moderately strong, positive logarithmic relationship between magnetic susceptibility and %TC for both cores ($r = 0.55$ avg. for cores 2 and 3; figure not shown). Lastly, there is a weak, positive linear relationship between %TOM and %TC ($r = 0.35$ avg. for cores 2 and 3; figure not shown).

Total inorganic phosphorus and aluminum (core LEGC03-3 only)

Total inorganic P (as defined by Aspila et al. 1976) averaged 779 ± 95 mg/kg through the entire LEGC03-3 core, or 86% of the total P in the sediments (Fig. 6). Total inorganic P is somewhat higher in the lower portion of the core than in the upper section. The greatest variability occurs between the core bottom and 450 cm. From 450 cm to 150 cm, the amplitude of variability decreases until the modern anthropogenic zone, which begins at 150 cm where the data are

Fig. 5 Core LEGC03-2 raw sediment data. From left to right: mass magnetic susceptibility; total organic matter; and, total carbonate

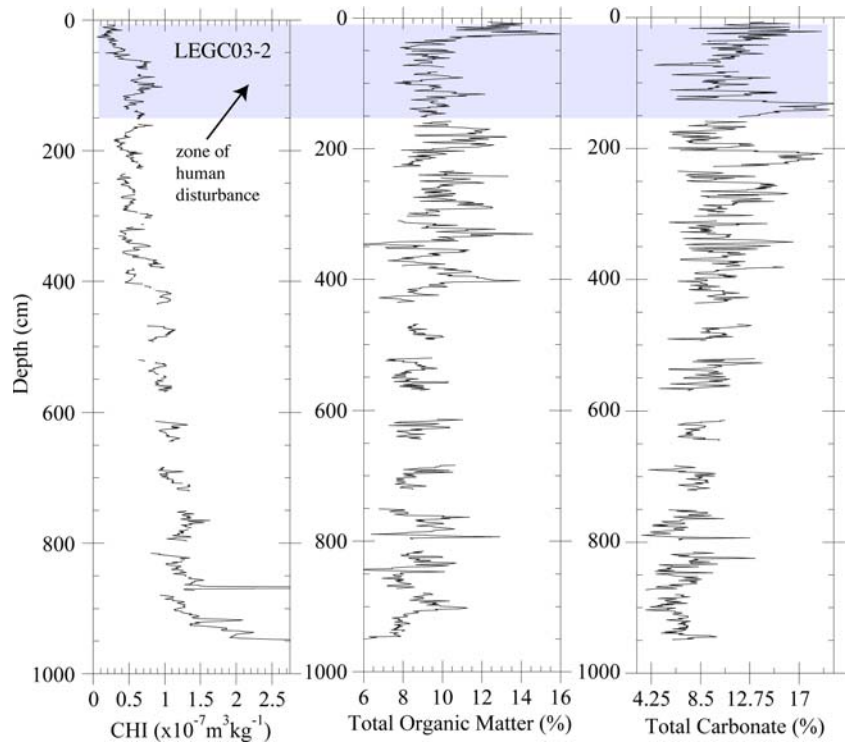
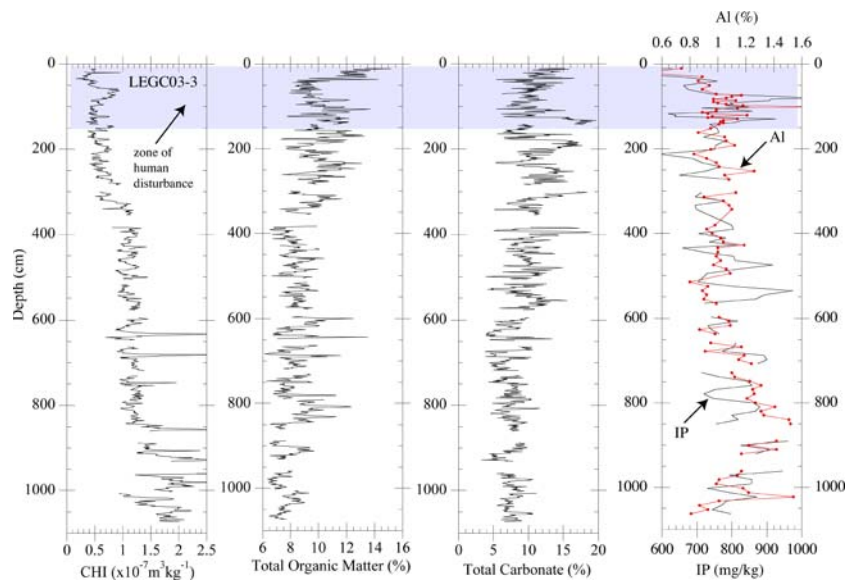


Fig. 6 Core LEGC03-3 raw sediment data. From left to right: mass magnetic susceptibility; total organic matter, total carbonate, % HCl-extractable Al; and, total inorganic phosphorus



characterized by large amplitude, high frequency variability (Fig. 6). The HCl-extractable Al averages 1.07% for the entire core (Fig. 6). The highest pre-anthropogenic Al values occur near the core bottom to a peak at 1,030 cm (Fig. 6). From 1,030 cm to 700 cm, the Al data are

characterized by a relatively smooth sinusoidal curve returning to lower values at 700 cm (Fig. 6). From 700 cm to 150 cm, %Al remains low with relatively subdued variability until concentrations increase dramatically in the anthropogenic zone, a time period that includes construction of the

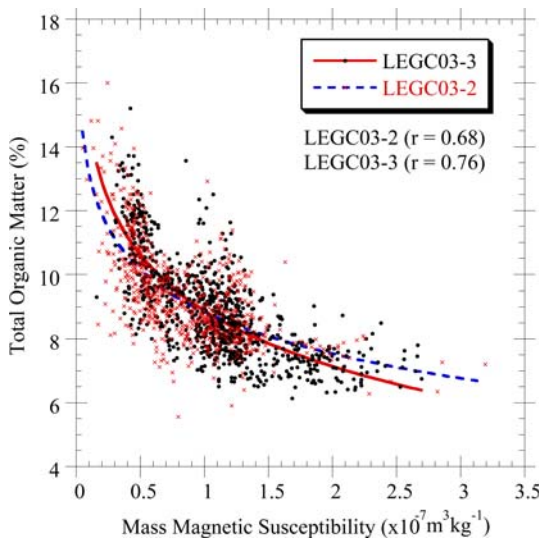


Fig. 7 Scatter diagram showing the relationships between mass magnetic susceptibility and total organic matter for both cores LEGC03-2 and LEGC03-3

Railroad Canyon Reservoir upstream of Lake Elsinore (1928) and extensive local and regional agricultural and municipal development. The total IP and %Al data are weakly, positively correlated throughout the core.

Composite core

One of this paper's objectives is to present the initial drill core results in the context of the composite core and its chronology. To accomplish this objective, we focused on the two cores extracted from the same deep basin—LEGC03-2 and -3 (Fig. 2). Our interpretation is that these two cores should contain similar sedimentologies assuming that the deep basin records whole lake process signals. Through the correlation of these cores, a single composite record is constructed in order to maximize the total length of sediment recovered for analysis.

The grey regions in Fig. 8 show the initial section correlations between cores LEGC03-2 and -3. White regions simply indicate intervals where no serious attempt was made to initially correlate the cores. The initial depth/depth correlation between cores LEG03-2 and LEG03-3 yields a r -values of 0.99, which indicates a constant proportion between sedimentation rates (Fig. 9).

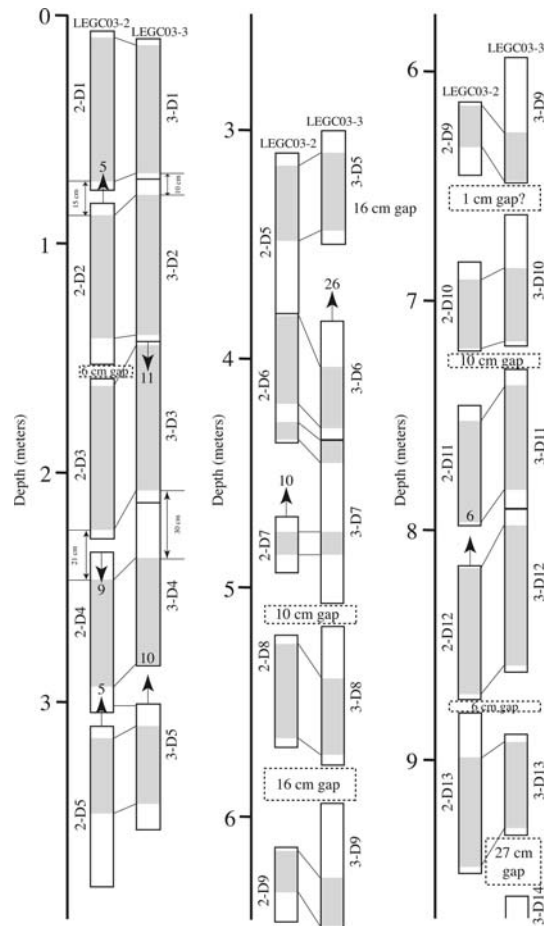


Fig. 8 Schematic illustrating the adjusted depth-depth correlation between LEGC03-2 and LEGC03-3. See text for more details

During the correlation process, it was apparent that ~ 10 cm errors could be made in the exact depth of each cored interval. Also, when sediment recovery in a segment was less than the interval cored, there was some uncertainty in exactly where the recovered sediment occurred within the cored interval. The correlations shown in Fig. 8 permitted us to revise slightly the stratigraphic depths of selected core segments to correct some of these errors. The logic used was that the two cores have almost identical sediment accumulation rates and thus the thickness of distinguishable intervals in one core should be comparable in the other core. For example, the gap between the base of correlations (grey interval) in segment 3-D1 (core LEG03-3 segment 1) and

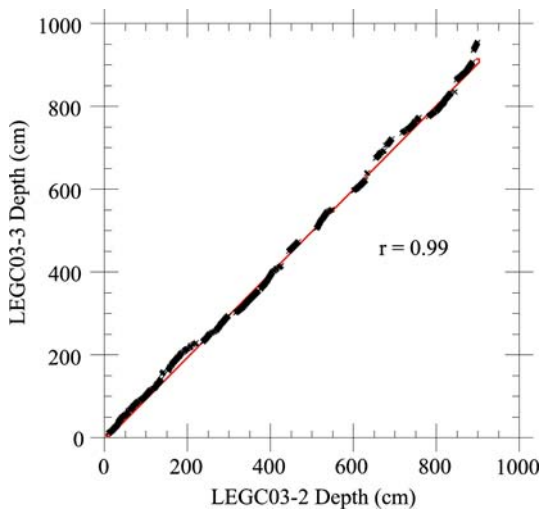


Fig. 9 Scatter diagram showing the tie-points using sediment description, mass magnetic susceptibility, total organic matter, and total carbonate for LEGC03-2 and LEGC03-3

the top of correlations in 3-D2 is 10 cm (Fig. 12). But, the gap between the equivalent base of correlations in 2-D1 and the top of correlations in 2-D2 is 15 cm (Fig. 8). There is a physical gap between segments 2-D1 and 2-D2 that would permit 2-D2 (and all core segments below it) to be raised by 5 cm (arrow with ‘5’ in Fig. 8). This change would make the gap between correlative horizons in the two cores the same, 10 cm. As another example, the gap between the base of correlative horizons in 3-D3 and the top of correlative horizons in 3-D4 is 30 cm (Fig. 8). The gap between the same correlative horizons in 2-D3 and 2-D4 is 21 cm (Fig. 8). If 2-D4, and all core segments below it, are lowered by 9 cm (arrow and ‘9’ in Fig. 8), then the gaps between the correlative horizons become the same thickness. In this way, the seven intervals indicated by arrows in Fig. 8 were revised. The overall effect of this stratigraphic revision was to shorten core LEG03-2 by 17 cm and core LEG03-3 by 25 cm. The effect of the revision is to make the cores appear even more similar in their overall sediment accumulation rates. The revised stratigraphic depths in core LEG03-3 and the equivalent revised depths based on correlation of core LEG03-2 to core LEG03-3 were used for all further analysis; this new composite core is

Table 2 Gaps in the composite Lake Elsinore record (core LEG03-3 revised depth scale)

GAP no.	Sediment interval	Data interval
1	0–6.5 cm (6.5)	0–8.5 cm (8.5)
2	147–153 cm (6)	141.9–153.1 cm (11.2)
3	481–491 cm (10)	480.5–493.5 cm (13.0)
4	552–568.5 cm (16.5)	551.5–569.5 cm (18.0)
5	636–637 cm (1)	634.5–637.5 cm (3.0)
6	694–704 cm (10)	693.5–706.5 (13.0)
7	836–843 cm (7)	835.5–843.8 cm (8.3)
8	907–934 cm (27)	906.5–934.5 cm (28.0)
9	978–981 cm (3)	977.5–981.5 cm (4.0)

hereafter referred to as composite core LEGC03. All data were averaged per depth between the two original cores when applicable; where sediment exists for one core only, the data for that core’s depth was used for the composite core. All final data, except IP and Al content, were smoothed with a 5-point running average for plotting (Table 2).

Age control

A total of 22 AMS ^{14}C dates and one cross-correlated pollen date from Kirby et al. (2004) were used in calculating an age model for composite core LEGC03 (Table 3; Fig. 10). All dates were converted to calendar years before present (hereafter cy BP) using CALIB 4.2.2 (Stuiver et al. 1998). Two dates were discarded based on their position relative to a known pollen age, correlated from core LESS02-11 to LEGC03-2 and LEGC03-3 using sediment descriptions, magnetic susceptibility, total organic matter, and total carbonate (see Kirby et al. 2004); two additional dates were also discarded because of their low $\delta^{13}\text{C}_{(\text{organic matter})}$ values, which suggested a re-worked origin. Dates not used in the calculation of the age model are also shown in Fig. 4 and Table 3. As shown by Kirby et al. (2004) surface sediments from the lake’s deepest basin provide a modern date; as a result, we do not consider our bulk sediment organic carbon dates to be affected significantly by old carbon. Precaution, however, was taken not to select sediment for dating from intervals interpreted as low stands to avoid obtaining false ages via obvious reworked older carbon (Kirby et al.

Table 3 Radiocarbon analyses^a not used in age model

Number	Core ID	Depth interval	Composite depth (cm)	UCIAMS ID	$\delta^{13}\text{C}$ (‰)	^{14}C AGE (BP)	\pm	Calendar Years BP ^a	2-Sigma range
1	LEG03-2	298–299	299.5	8260	-17.8	2,290	20	2,330	2,307–2,348
2	LEG03-2	405–406	396.5	6832	-21.0	2,075	25	2,060	1,987–2,123
3	LEG03-2	405–406	396.5	6695	-14.2	2,060	35	2,030	1,932–2,122
4	LEG03-2	432–433	421.93	8261	-16.2	2,915	25	3,020	2,957–3,081
5	LEG03-2	556–557	533.79	8262	-15.2	4,385	30	4,930	4,864–4,996
6	LEG03-2	624–625	614.17	6833	-15.8	4,605	25	5,420	5,396–5,449
7	LEG03-2	850–851	818.69	6834	-14.4	6,825	30	7,650	7,606–7,697
8	LEG03-2	947–948	899	6835	-17.7	7,350	30	8,160	8,106–8,196
9 ^a	LEG03-3	105–106	105.5	8263	-20.7	860	25	740	694–794
10 ^a	LEG03-3	162–163	173.5	8264	-20.4	650	20	580	559–602
11	LEG03-3	195–196	206.5	8265	-17.9	1,180	20	1,110	1,055–1,171
12	LEG03-3	264–265	275.5	8266	-17.5	1,115	25	1,010	962–1,062
13	LEG03-3	324–325	325.5	8267	-18.4	2,270	30	2,220	2,179–2,265
14	LEG03-3	395–396	370.5	8268	-20.3	2,610	20	2,750	2,734–2,774
15	LEG03-3	469–470	444.5	8270	-17.6	3,160	25	3,400	3,341–3,453
16	LEG03-3	536–537	511.5	8271	-19.2	3,125	20	3,350	3,321–3,385
17 ^a	LEG03-3	610–611	585.5	8272	-16.1	5,160	30	5,920	5,888–5,950
18	LEG03-3	635–636	610.5	8274	-18.4	4,955	30	5,670	5,609–5,735
19	LEG03-3	683–684	658.5	8275	-18.1	4,945	30	5,670	5,606–5,728
20	LEG03-3	713–714	688.5	8277	-17.6	6,025	35	6,850	6,745–6,949
21	LEG03-3	759–760	734.5	8278	-17.3	5,820	30	6,610	6,532–6,679
22	LEG03-3	800–801	775.5	8279	-18.1	5,540	40	6,340	6,279–6,407
23	LEG03-3	924–925	899.5	8280	-19.4	7,910	50	8,700	8,595–8,813
24 ^a	LEG03-3	986–987	961.5	8283	-14.9	8,465	40	9,500	9,464–9,532
25	LEG03-3	1048–1049	1023.5	8284	-17.0	8,225	40	9,180	9,057–9,301
26	LEG03-3	1071–1072	1046.5	8286	-18.0	7,965	40	8,850	8,695–8,999

^a Calib 4.2.2 Stuiver et al. (1998)

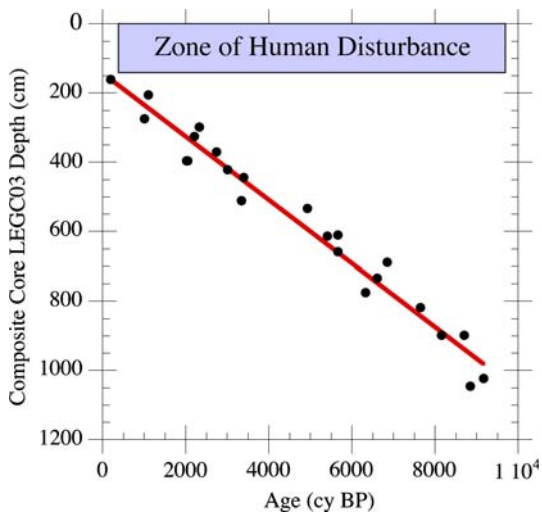


Fig. 10 Age model for composite core LEGC03. Age model for the past 200 calendar years is from Kirby et al. (2004)

2004; Smoot and Benson 2004). Even with careful sampling, it is apparent that some reworking of older material occurs in the lake basin as shown by the occasional age reversals (Fig. 4).

The purpose of an age model is to assign an absolute date to each depth of analysis. In turn, the data are compared to age directly. For this research we chose to use a single “best-fit” line to create an age model. The breadth of scatter (Fig. 10) is large enough to preclude a more precise point-by-point linear fit. For our age model, a simple linear fit is used ($r = 0.98$). A pollen age cross-correlated from LESS02-11 (see Kirby et al. 2004) provides the upper boundary to our age model at 200 ± 20 cy BP at 161 cm in composite core LEGC03. The best-fit line overestimates the pollen age by 153 years. To accommodate this over-estimation, 153 years were subtracted to each date in the age model starting after the 200 cy BP age-depth. Furthermore, we recognize the temporal limitations of our age

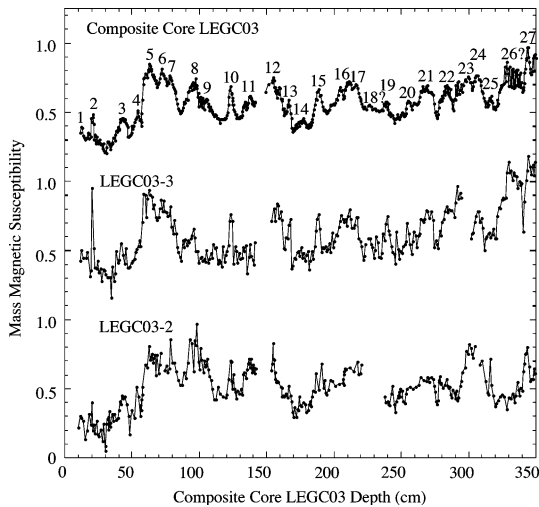


Fig. 11 Comparison illustrating centimeter scale mass magnetic susceptibility data for composite core LEGC03 and corrected depths for LEGC03-2 and LEGC03-3 between 0 cm and 350 cm

model due to the scatter of the ages and possible occurrence of sediment hiatuses or slow deposition during low lake levels. As a result, we feel that our proxy data using this age model are, at best, resolving multi-decadal-to-centennial scale variability. The centimeter scale cross-correlation supports this contention that the sediments truly record high-resolution, multi-decadal-to-centennial scale event stratigraphy (Fig. 11). Figure 11 shows an example of the centimeter-scale, cross-core correlation using magnetic susceptibility between 0 cm and 350 cm; a similar level of centimeter scale, cross-correlation exists for the intervals 350–950 cm (data not shown). Although not shown, both total organic matter and total carbonate show similar centimeter scale cross-correlations. This centimeter-scale coherency adds confidence to our interpretation that the composite core LEGC03 records fine-scale event stratigraphy when transferred to the age model.

Discussion

Proxy interpretations

For this research, a combination of a six sediment-based proxies are used to infer climate

change. These proxies include sediment description, mass magnetic susceptibility, % total organic matter, % total carbonate, % HCl-extractable Al, and total inorganic P.

Sediment lithology is a commonly used and powerful descriptive proxy for interpreting climate change from lake sediments (e.g. Hardie et al. 1978; Plummer and Gostin 1981; Rosen 1991; Smoot 1991; Hovorka 1997; Last and Vance 1997; Smoot and Benson 1998; Negrini et al. 2006). Similar to the latter papers, we interpret mud cracks as direct evidence for desiccation. Intervals of complex sediment structures including possible mud cracks, rotational features associated with drying/wetting, burrows and/or distinct bioturbation are also interpreted as evidence for low lake levels and/or possible desiccation. Massive sediment with no evidence for subaerial exposure is interpreted as evidence for deeper lake levels. Thin silt layers are interpreted as rapid depositional features associated with storms events.

Magnetic susceptibility is a measure of the amount of magnetic minerals in a sediment sample (Thompson et al. 1975; Gale and Hoare 1991). As a climate proxy, magnetic susceptibility of lake sediments can reflect a variety of processes, which are often related to variations in sediment source (Baker et al. 2001; Armour et al. 2002; Jenkins et al. 2002) and/or changes in sediment flux (Cioppa and Kodama 2003; Brown et al. 2002; Seltzer et al. 2002). Under certain chemical conditions, post-depositional processes confound the primary magnetic signal. These processes can either enhance or suppress the original magnetic signal (Hilton and Lishman 1985; Reynolds and King 1995; Tarduno 1995; Reynolds et al. 1999; Geiss et al. 2004; Peck et al. 2004). For this paper, we suggest that magnetic susceptibility is a proxy for relative lake level or climate wetness, similar to Kirby et al. (2004). Kirby et al. (2004) explain the positive relationship between lake level and magnetic susceptibility through changes in the flux of magnetic detritus in response to changing precipitation amounts. In support of this hypothesis, Inman and Jenkins (1999) show a strong positive relationship between climate wetness and river sediment flux over the 20th century. This observation between

high (low) magnetic susceptibility and high (low) lake level has been previously noted; however, the underlying mechanism relating the two variables may vary from basin to basin (Benson et al. 1998; Negrini et al. 2000). Alternatively, simple dilution by organics and carbonates may also play an important role in determining the magnetic susceptibility of the lake sediments. There is a strong inverse relationship between total organic matter and magnetic susceptibility; the same relationship is true for total carbonate and magnetic susceptibility (Fig. 7). Higher productivity and carbonate production during lower, or lowering, lake levels may dilute the magnetic susceptibility signal. The magnetic susceptibility signal may also reflect enhanced dissolution or diagenesis under reducing conditions caused by higher organic matter rather than changes in sediment run-off. Regardless of the above scenario, the net effect—either through a change in sediment flux, dilution, or dissolution—is to change magnetic susceptibility in the same direction (i.e., wet (dry) climate = higher (lower) magnetic susceptibilities). As a result, magnetic susceptibility is interpreted as a proxy for relative climate wetness/lake level.

Total organic matter through loss-on-ignition at 550°C is an easily analyzed and insightful measurement for lake paleoclimate studies (Dean 1974; Heiri et al. 2001). In lake systems, total organic matter reflects a combination of autochthonous and allochthonous sources. Allochthonous organic matter derives from terrestrial organic matter, which is eroded into the lake basin. The total contribution of allochthonous organic matter is controlled by several factors including drainage basin flora, regional climate, and basin topography (Meyers and Ishiwatari 1993). In most lakes, except for extremely oligotrophic lakes, the autochthonous source dominates (Dean and Gorham 1998). Autochthonous organic matter derives from in situ lake productivity of various types (Meyers and Ishiwatari 1993). The amount of autochthonous organic matter in lake systems is often related to water temperature, water column turbidity, and/or nutrient availability (Dean 1981; Benson et al. 1998; Willemse and Tornqvist 1999; Kirby et al. 2005). CN data from Anderson (2001) show that

autochthonous lake organic matter constitutes the primary source of organic matter in Lake Elsinore. Furthermore, Anderson (2001) has shown that internal nutrient loading dominates nutrient availability and thus productivity levels in modern Lake Elsinore. Anderson (2001) concludes that lower lake levels enhance the effect of both wind-driven resuspension and bioturbation, both of which enhance internal nutrient loading and lake productivity. Using this modern lake study, we interpret total organic matter as a proxy for lake level change over the Holocene. In other words, lower (higher) lake levels produce higher (lower) total organic matter through a combination of enhanced internal nutrient loading through wind-driven resuspension and/or bioturbation in the shallow to moderate lake regions.

Total carbonate determined through loss-on-ignition at 950°C is also an easily analyzed and insightful measurement for lake paleoclimate studies (Dean 1974; Heiri et al. 2001). Sediment carbonate in lake systems is produced within the lake through a variety of possible processes (Thompson et al. 1997; Mullins 1998; Hodell et al. 1998; Benson et al. 2002; Kirby et al. 2002b). Because there is no significant local source of detrital carbonate within Lake Elsinore's drainage basin, it is assumed that the carbonate in the lake's sediment is entirely autochthonous (Engel 1959); although, the influence of wind-blown carbonate dust cannot be ruled out at this point (Reheis and Kihl 1995). In addition, we cannot rule out mixing of waters with different source areas as a cause of changes in the relative saturation of lake waters with respect to calcium carbonate. In the modern lake system, Anderson (2001) has shown that carbonate precipitates directly within the water column in response to CO₂ drawdown by phytoplankton. There is also a strong seasonal contrast in carbonate precipitation that indicates a temperature role. Furthermore, hydrologic models by Anderson (2001) show that carbonate precipitation will increase as lake-levels decrease in response to saturation of the water column with respect to calcium and carbonate. Similar to the total organic matter, we interpret total carbonate as a proxy for relative lake level (i.e., high (low) carbonate = low (high) lake levels).

Two additional sediment analyses, % HCl-extractable Al and total inorganic P, were also used to infer past climate conditions. Extraction of sediments with 1 M HCl was originally proposed by Aspila et al. (1976) for the measurement of inorganic P. Although operationally defined, the extraction process is thought to recover most inorganic forms of P in sediments, including P associated with iron and aluminum oxyhydroxides, calcium carbonate, apatite and other phases; it is not effective at solubilizing P within crystalline silicate minerals. Extraction with 1 M HCl has also been recommended by the ASTM D3974-81 Practice B (ASTM 1990) for the recovery of bioavailable forms of metals and trace elements in sediments. In this study, we used 1 M HCl extractions to quantify both total inorganic P and extractable Al contents in the sediments. Numerous researchers use this extraction procedure to quantify the concentrations of inorganic/organic P and Al in lake, marine, and suspended sediments (e.g. Gunatilaka 1991; Rees et al. 1991; Johnson et al. 2002; Vaalgamaa 2004). For example, Berner and Rao (1994) found that ~70% of the P in the suspended sediment of the Amazon River was in an inorganic form and that the organic forms of P were lost during early diagenesis while inorganic P was not altered; although, some net transfer of P from organic to inorganic forms occurs with increased time. Here, we interpret total inorganic P and extractable Al as relative measures of material derived principally from lithogenic sources (e.g. Hamilton et al. 2001). Therefore, total inorganic P and extractable Al are interpreted as proxies for relative climate wetness and local run-off of weathered/eroded lithogenic material (i.e., wetter climate/more run-off = higher IP and %Al and vice versa).

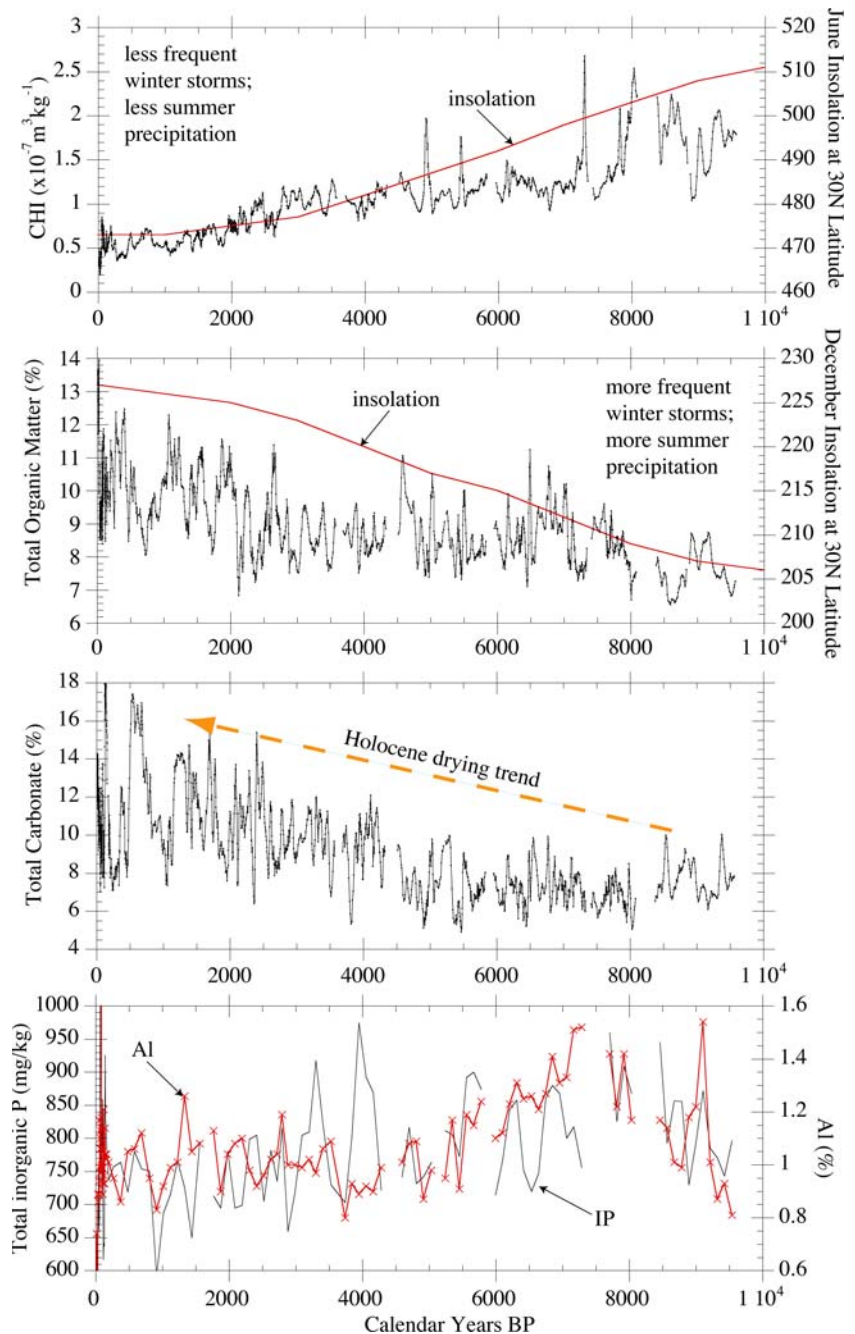
Insolation forcing of Holocene climate in Southern California

Over the past 10,000 calendar years, hydrologic variability in Southern California has been controlled by two primary forcings: insolation (incoming solar radiation due to earth–sun orbital parameters—Milankovitch forcing) and waning glacial conditions (i.e. retreat of continental ice

sheets in North America). Ice sheet dynamics affect Southern California through its modulation of atmospheric circulation as the ice front advances and retreats (e.g. see Negrini 2002). For this research, the impact of the North American ice sheets is minimal because the vast majority had disintegrated by 10,000 cy BP in western North America, or the start of the Lake Elsinore record presented in this study. Insolation, on the other hand, is an entirely external driver of the earth's climate system. Therefore, insolation should be one of the primary drivers of Holocene climate variability for almost any geographic location (Kutzbach 1981; Kutzbach and Guetter 1986; Kutzbach and Gallimore 1988; Harrison et al. 2003; Diffenbaugh and Sloan 2004; Wohlfahrt et al. 2004; Lorenz et al. 2006). Insolation drives climate through its affect on the strength of seasonality (e.g. monsoonal circulation: Kutzbach 1981; Kutzbach and Guetter 1986; Harrison et al. 2003), the mean position of the polar front jet stream (Kirby et al. 2002a, b), and its associated storm tracks (e.g. Sawada et al. 2004). Therefore, it is our hypothesis that changes in winter/summer insolation are the primary forcing of long-term Holocene climate change in Southern California. The idea of a connection between insolation and Holocene climate has been suggested elsewhere (e.g. Baker et al. 2001; Abbott et al. 2003; McFadden et al. 2005; Lorenz et al. 2006). In fact, Kirby et al. (2005) has previously suggested this relationship in Southern California using low-resolution sediment cores from Lake Elsinore's littoral zone. In this paper, we re-visit this insolation hypothesis using higher resolution, intact and complete Holocene sediment cores from Lake Elsinore's modern depocenter.

As previously stated, insolation has changed over the course of the Holocene. Today's winter and summer insolation values are 9% higher and 7% lower than 10,000 years ago, respectively (Fig. 12). It is well documented that greater summer insolation in southwestern North America increases the magnitude and spatial extent of the North American monsoon (NAM hereafter), generally manifest as local convective thunderstorms (Tubbs 1972; Mitchell et al. 2002; Spaulding 1990; Liu et al. 2003).

Fig. 12 Composite core LEGC03 age model and sediment data with relevant climate features as mentioned in the text. AI and IP data are from core LEGC03-3 only and are transferred to the composite core depth scale. Insolation values from Berger (1978)



Higher summer insolation should also favor an increase in the frequency of occasional, land-falling tropical cyclones in Southern California. Global circulation models used to reconstruct early Holocene climate consistently show greater than modern summer, and total, precipitation in response to higher summer insolation and its modulation of regional monsoonal circulation

(Kutzbach 1981; Kutzbach and Guetter 1986; Kutzbach and Gallimore 1988; Diffenbaugh and Sloan 2004). It is also suggested that lower winter insolation favors an increase in the frequency of winter storms across southwest North America in response to a lower latitude polar front jet stream position (e.g. Kirby et al. 2005).

Two early Holocene sediment records from Dry Lake (Filippelli and Souch 1999; Filippelli et al. 2000; Bird and Kirby 2006), a cosmogenically dated glacial record from the Dry Lake area (Owen et al. 2003), a low resolution littoral record from Lake Elsinore (Kirby et al. 2005), and a 7,000 year marsh record from San Joaquin Marsh (Davis 1992) all favor the interpretation that the early Holocene was wetter than today (Fig. 1). Kirby et al. (2005) and Bird and Kirby (2006) argue that greater early Holocene summer insolation enhanced the magnitude and spatial extent of the NAM as well as the occurrence of tropical cyclones. Combined with lower winter insolation, which would have increased the frequency of winter storms across the study region, there should be an expected rise in total annual precipitation, thus favoring sustained, deep lakes. As a result, it is our position that Southern California, which today is minimally influenced by the NAM and rarely affected by tropical cyclones, was impacted more frequently in the early Holocene by each of these late summer–early fall systems. And, because the NAM is regionally characterized by short-lived, strong convective thunderstorms, particularly in the mountains where Dry Lake located (i.e., San Bernardino Mtns. in the Transverse Range), it is often associated today with flash floods and significant local erosion (Tubbs 1972). In both Dry Lake records and the low resolution Lake Elsinore record, the authors observe distinct storm sediment facies, chemical constituents, and/or sediment deposited by more vigorous hydrologic processes during the early Holocene (Filippelli and Souch 1999; Filippelli et al. 2000; Kirby et al. 2005; Bird and Kirby 2006). Owen et al. (2003) cosmogenically dated glacial record from the Dry Lake area dates a small glacial advance in the early to mid Holocene. Bird and Kirby (2006) attribute this glacial advance to the proposed 8.2 ka cold event (Barber et al. 1999). However, the entire early Holocene as revealed in the Dry Lake sediment record indicates a substantially wetter climate than today both before and after the so-called 8.2 ka cold event (Bird and Kirby 2006). The San Joaquin Marsh record also indicates a wetter early–mid Holocene than today based on the occurrence of freshwater pollen (Davis 1992).

Similar to the Southern California, early Holocene paleoclimate records discussed above, the new Lake Elsinore, high-resolution sediment record presented in this study also favors an interpretation of a wetter early Holocene. Lithologic descriptions for cores LEGC03-2 and -3 show a preponderance of silty “storm layers” during the early-to-mid-Holocene (Fig. 4). The early Holocene sediments are also a largely homogenous clays with no evidence for sustained desiccation (i.e., mud cracks or deep bioturbation via roots). Total organic matter and total carbonate are both lowest in the early Holocene (Fig. 12). In congruence with our proxy interpretation, it is suggested that lower total organic matter and total carbonate values reflect a decrease in lake productivity in response to a higher lake level. According to Anderson (2001), a deeper lake should reduce internal nutrient loading, which is essential in Lake Elsinore to primary productivity, by diminishing the effect of wave action resuspension and bioturbation. And, because carbonate production is linked to primary productivity through photosynthetic draw-down of CO₂, carbonate production within the water column should also decrease in response to lower productivity caused by lower nutrient concentrations in response to higher lake levels. Conversely, magnetic susceptibility is characterized by the highest average values in the early Holocene. These high magnetic susceptibility values may reflect either, or a combination of, enhanced erosion in response to a wetter climate, reduced magnetic mineral dissolution and alteration due to lower total organic matter, or a simple decrease in dilution in association with lower total organic matter and total carbonate. In any case, these interpretations of magnetic susceptibility agree with the sedimentological and the total organic matter/total carbonate interpretations, which imply a wetter early Holocene. In addition, Al content and total inorganic phosphorus, both interpreted as derived from eroded lithogenic material, are highest in the early Holocene supporting our interpretation that the early Holocene was wetter than present (Fig. 12).

Similar to the interpretation of Kirby et al. (2005) and Bird and Kirby (2006), the wetter-than-today early Holocene climate in Southern

California is attributed to insolation forcing. Lower winter insolation in the early Holocene likely increased the frequency of winter storms across the study region. From modern lake level–precipitation analyses of Lake Elsinore, it is apparent that a slight increase in winter storm activity produces a significant impact on the lake’s depth (Fig. 3; Hudson 1978). Combined with the proposed increase in late-summer/early-fall precipitation, perhaps linked to a more spatially expansive and greater magnitude NAM as well as a concomitant increase in the occasional land-falling tropical cyclone, the net result is to increase total annual precipitation, which creates optimum conditions for a wet early Holocene.

Following the wet early Holocene climate, all proxy data from composite core LEGC03, including the physical sedimentology, indicate a long term Holocene drying (Figs. 4, 12). Only in the latest Holocene, however, is there evidence in the form of sedimentary structures for sustained drying events or low lake level (e.g. mud cracks, distinct bioturbation, rotational features). Despite the occurrence of these structures, and perhaps due to limited age resolution, we cannot conclude that any significant sediment hiatuses exist. Certainly, we do not see any evidence for the prolonged mid-Holocene drying (i.e., desiccation) events that characterize Pyramid Lake (Benson et al. 2002), Owens Lake (Benson et al. 2002), Walker Lake (Benson et al. 1991), and Lake Tahoe (Lindstrom 1990). Both total organic matter and total carbonate increase slowly over the Holocene, which are interpreted to reflect lower lake level and its effect on moderating lake productivity through internal nutrient loading. The rise in total carbonate in the sediments may also indicate an increase in precipitation of CaCO_3 within the water column due to evapoconcentration of Ca^{2+} and CO_3^{2-} as lake levels decreased in response to less total precipitation (Fig. 12). Al content and total inorganic phosphorus decline over the Holocene perhaps in response to a drier climate and a reduction in drainage basin erosion and/or dilution due to increased autochthonous organic matter and carbonate production. Noteworthy is the strong correlation between total organic matter and total carbonate (r^2 of 0.55), while no correlation is present between total organic matter and inorganic

P (r^2 of 0.05). This lack of correlation of the latter supports our interpretation that inorganic P concentrations reflect changes in the amount of eroded lithogenic materials rather than simple dilution by higher organic matter and carbonates. Magnetic susceptibility also decreases over the Holocene. Here again, however, it is not clear if this decrease in magnetic susceptibility is due to a decrease in run-off, dilution, or enhanced alteration in the presence of higher total organic matter. Nonetheless, when taken together, the six proxies above are explained, with the least controversy, as evidence for a long term Holocene drying. Similar to the Lake Elsinore record, both the Dry Lake (Bird 2005) and the San Joaquin Marsh records show evidence for a long term Holocene drying trend.

Here again, insolation forcing is used to explain this Holocene-length climate trend (Fig. 12). Summer insolation steadily decreased over the past 10,000 years reducing the impact and spatial extent of the North American Monsoon and the occasional land-falling tropical cyclone. As a result, only the mountainous regions and deserts of Southern California receive occasional monsoonal rains in the present climate regime (Tubbs 1972; Bird and Kirby 2006). At the same time, winter insolation increased. Although slight, this steady increase in winter insolation may have reduced the frequency of large winter storms across the study region. Again, as shown by an analysis of modern lake level–precipitation relationships, a slight decrease in winter precipitation can lead to a rapid lowering of lake level (Fig. 3; Hudson 1978). As a result, it is hypothesized that the combined reduction of summer and winter precipitation through insolation changes produced a long term Holocene drying as recorded in sediments from Lake Elsinore.

Regional comparison

For a regional comparison, we focus on three terrestrial sites surrounding Southern California, which contain well-dated, climate records: (1) the southern Great Valley (Tulare Lake); (2) southern Sierra Nevadas (Owens Lake); and, (3) the Mojave Desert (Silver Lake and Soda Lake) (Fig. 1). Our comparison is not bounded to the south (i.e., Baja) because there are no known,

well-dated early Holocene, terrestrial records from the region for comparison.

The reason for focusing on the three terrestrial paleoclimate records above is that each of the sites selected contain well-dated paleo-lake level reconstructions. Admittedly, there are a variety of proxies used for inferring past climate. However, paleo-shoreline, raised lacustrine sediments, and raised deltas provide one of the only ways to quantify, volumetrically, “how wet” past climates were when compared to present climate. At Tulare Lake, a recent lake level reconstruction using paleo-shoreline features tied to depocenter sediment cores indicates that the highest Holocene lake level occurred between 9,400 and 8,200 cy BP (Negrini et al. 2006). Two additional near high stands occurred at 10,000 cy BP and between 7,000 and 6,500 cy BP at Tulare Lake (Negrini et al. 2006). A methodologically similar study at Owens Lake using raised fluvio-deltaic and lacustrine sediments also indicates that the highest Holocene lake level occurred in the early Holocene between 10,000 and 8,000 cy BP (Bacon et al. 2006). From the Mojave region, paleo-shoreline features and depocenter sediment core stratigraphies from Silver Lake, the terminal basin of the Mojave River, indicate permanent lake conditions until sometime between 8.7 ka and 9.3 ka (Wells et al. 2003). Together, these three regionally disparate study sites support our interpretation that the early Holocene was wetter than today, and perhaps, the wettest of the Holocene. Each of these records also indicate a general decrease in lake level over the Holocene; although, there are occasional high stands, but none as high as the early Holocene.

The region included in this comparison represents both a spatially diverse assemblage and a climatically complex region. As a result, these near contemporaneous records of a wetter-than-modern early Holocene followed by a drying trend require a forcing that is independent of regional-scale idiosyncrasies. We suggest that insolation forcing, and its affect on the seasonality of precipitation, explains best the wet early to dry late-Holocene trend. Future research will evaluate sub-orbital scale climate change for the region to

determine the spatial and temporal phasing of higher-frequency climate change and its potential forcings.

Conclusions

A composite drill core from Southern California’s largest, natural lake—Lake Elsinore—reveals a wetter-than-modern early Holocene followed by long-term Holocene drying trend. The wetter-than-modern early Holocene is attributed to changes in winter/summer insolation. These changes increased the frequency of winter storms and the spatial extent/magnitude of the NAM. It is also possible that higher early Holocene summer insolation favored an increase in the occasional land-falling tropical cyclone. The long-term drying trend is a potentially linear response to changing summer/winter insolation and its modulation of seasonal precipitation variability. The results from Lake Elsinore are supported locally by Dry Lake sediment and glacial records as well as by the San Joaquin Marsh sediment record. Regionally, the Lake Elsinore paleoclimatic interpretations are supported by paleo-lake level reconstructions from Tulare Lake, Owens Lake, and Silver Lake, which indicate the highest lake levels in the early Holocene followed by a general decline.

As a side note, Berger and Loutre (2002) suggest that our present interglacial may be longer than previously thought in response to less variable insolation. If their hypothesis is correct, our data indicate that Southern California may be especially sensitive to insolation forcing and may therefore experience continued drying well into the future with severe implications for population growth and water availability.

Acknowledgements The authors thank the Lake Elsinore-San Jacinto Water Authority (LESJWA) for funding this drill core project and its analyses (to MEK, MAA); the City of Lake Elsinore, particularly Mr. Patrick Kilroy (Lake Manager) for access to the lake; Mr. David Ruhl for contract management; Gregg Drilling for exceptional quality service; Drs. John Southon and Guaciara dos Santos (Univ. of Cal. Irvine) for radiocarbon dating; ACS-PRF Grant #41789-GB8 (to MEK); and, Ms. Jennifer Schmidt for careful lab analyses. The comments of three anonymous reviewers and the editor helped to improve the manuscript’s clarity and content; their time and thoughtful comments are greatly appreciated.

References

- Abbott MB, Aravena R, Mark BG, Polissar PJ, Rodbell DT, Rowe HD, Vuille M, Wolfe BB, Wolfe AP, Seltzer GO (2003) Holocene paleohydrology and glacial history of the central Andes using multiproxy lake sediment studies. *Palaeogeogr Palaeoclimatol Palaeoecol* 194:123–138
- Adams DK, Comrie AC (1997) The North American monsoon. *Bull Am Meteorol Soc* 78:2197–2213
- Anderson MA (2001) Internal loading and nutrient cycling in Lake Elsinore. Final Report for Santa Ana Regional Water Quality Control Board, Lake Elsinore, 52 pp
- Anderson WT, Mullins HT, Ito E (1997) Stable isotope record from Seneca Lake, New York: evidence for a cold paleoclimate following the Younger Dryas. *Geology* 25:135–138
- Anonymous (1979) Aquifer exploration at Lake Elsinore. *Pac Grou Dig*:10–12
- Armour J, Fawcett PJ, Geissman JW (2002) 15 k.y. paleoclimatic and glacial record from northern New Mexico. *Geology* 30:723–726
- Aspila KI, Agemian H, Chau ASY (1976) A semi-automated method for the determination of inorganic, organic and total phosphate in sediments. *Analyst* 101:187–197
- ASTM (American Society for Testing and Materials) (1990) Standard practices for extraction of trace elements from sediments, D3974-81
- Bacon SN, Burke RM, Pezzopane SK, Jayko AS (2006) Last glacial maximum and Holocene lake levels of Owens Lake, eastern California, USA. *Quat Sci Rev* 25:1264–1282
- Baker PA, Grove MJ, Tapia PM, Cross SL, Rowe HD, Broda JP, Seltzer GO, Fritz SC, Dunbar RB (2001) The history of South American tropical precipitation for the past 25,000 years. *Science* 291:640–643
- Barber DC, Dyke A, Hillaire-Marcel C, Jennings AE, Andrews JT, Kerwin MW, Bilodeau G, McNeely R, Southon J, Morehead MD (1999) Forcing of the cold event of 8,200 years ago by catastrophic drainage of Laurentide lakes. *Nature* 400:344–347
- Benson L, Lund S, Paillet F, Smoot J, Kester C, Mensing S, Meko D, Lindström S, Kashgarian M, Rye R (2002) Holocene multidecadal and multicentennial droughts affecting Northern California and Nevada. *Quat Sci Rev* 21:659–682
- Benson LV, Meyers PA, Spencer RJ (1991) Change in the size of Walker Lake during the past 5000 years. *Palaeogeogr Palaeoclimatol Palaeoecol* 81:189–214
- Benson LV, Phillips FM, Rye RO, Burdett JW, Kashgarian M, Lund SP (1996) Climatic and hydrologic oscillations in the Owens Lake Basin and adjacent Sierra Nevada, California. *Science* 274:746–749
- Benson LV, May HM, Antweiler RC, Brinton TI, Kashgarian M, Smoot JP, Lund SP (1998) Continuous lake-sediment records of glaciation in the Sierra Nevada between 52,600 and 12,500 ¹⁴C yr B.P. *Quat Res* 50:113–127
- Berger AL (1978) Long-term variations of daily insolation and Quaternary climatic changes. *J Atmos Sci* 35:2361–2367
- Berger A, Loutre MF (2002) An exceptionally long interglacial ahead? *Science* 297:1287–1288
- Berner RA, Rao JL (1994) Phosphorus in sediments of the Amazon River and estuary: implications for the global flux of phosphorus to the sea. *Geochim Cosmo Acta* 58:2333–2339
- Beuhler M (2003) Potential impacts of global warming on water resources in Southern California. *Water Sci Technol* 47:165–168
- Biondi F, Gershunov A, Cayan DR (2001) North Pacific decadal climate variability since 1661. *J Clim* 14:5–10
- Bird BW (2005) A 9,000 year record of long-term climate change and abrupt climate events from Dry Lake, Southern California. MSc Thesis, California State University at Fullerton, 90 pp
- Bird BW, Kirby ME (2006) An alpine lacustrine record of early Holocene North American Monsoon dynamics from Dry Lake, Southern California (USA). *J Paleolimnol* 35:179–192
- Brown S, Bierman P, Lini A, Davis PT, Southon J (2002) Reconstructing lake and drainage basin history using terrestrial sediment layers: analysis of cores from a post-glacial lake in New England, USA. *J Paleolimnol* 28:219–236
- Byrne R, Reidy L, Kirby M, Lund S, Poulsen C (2003) Changing sedimentation rates during the last three centuries at Lake Elsinore, Riverside County, California, Final Report for the Santa Ana Regional Water Quality Control Board, 41 pp
- Cayan DR, Dettinger MD, Diaz HF, Graham NE (1998) Decadal variability of precipitation over Western North America. *J Clim* 11:3148–3166
- Cayan DR, Roads JO (1984) Local relationships between United States West Coast precipitation and monthly mean circulation parameters. *Mon Weath Rev* 112:1276–1282
- Cioppa MT, Kodama KP (2003) Environmental magnetic and magnetic fabric studies in Lake Waynewood, northeastern Pennsylvania, USA: evidence for changes in watershed dynamics. *J Paleolimnol* 29:61–78
- Cole KL, Wahl E (2000) A late Holocene paleoecological record from Torrey Pines State Reserve, California. *Quat Res* 53:341–351
- D'Arrigo R, Villalba R, Wiles G (2001) Tree-ring estimates of Pacific decadal climate variability. *Clim Dyn* 18:219–224
- Damiata BN, Lee TC (1986) Geothermal exploration in the vicinity of Lake Elsinore, Southern California. *Geother Res Coun Trans* 10:119–123
- Davis OK (1992) Rapid climatic change in coastal Southern California inferred from pollen analysis of San Joaquin Marsh. *Quat Res* 37:89–100
- Dean WE (1974) Determination of carbonate and organic matter in calcareous sedimentary rocks by loss on ignition: comparison with other methods. *J Sed Pet* 44:242–248

- Dean WE (1981) Carbonate minerals and organic matter in sediments of modern north temperate hard-water lakes. In: Ethridge FG, Flores RM (eds) Recent and ancient nonmarine depositional environments: models for exploration. Society of Economic Paleontologists and Mineralogists, Tulsa, Special Publication 31, pp 213–231
- Dean WE, Gorham E (1998) Magnitude and significance of carbon burial in lakes, reservoirs, and peatlands. *Geology* 26:535–538
- Dettinger MD, Cayan DR, Diaz HF, Meko DM (1998) North–South precipitation patterns in western North America on interannual-to-decadal timescales. *J Clim* 11:3095–3111
- Diffenbaugh NS, Sloan LC (2004) Mid-Holocene orbital forcing of regional-scale climate: a case study of Western North America using a high-resolution RCM. *J Clim* 17:2927–2937
- Douglas AV, Cayan DR, Namias J (1983) Large-scale changes in North Pacific and North American weather pattern in recent decades. *Mon Weat Rev* 110:1851–1862
- Douglas MW, Maddox RA, Howard K, Reyes S (1993) The Mexican Monsoon. *J Clim* 6:1665–1677
- Drummond CN, Patterson WP, Walker JCG (1995) Climatic forcing of carbon–oxygen isotopic covariance in temperate region marl lakes. *Geology* 23:1031–1034
- Engel R (1959) Geology of the Lake Elsinore quadrangle, California. California Geological Survey, Santa Ana
- Enzel Y, Brown WJ, Anderson RY, McFadden LD, Wells SG (1992) Short-duration Holocene lakes in the Mojave River drainage basin, Southern California. *Quat Res* 38:60–73
- Filippelli GM, Souch C (1999) Effects of climate and landscape development on the terrestrial phosphorus cycle. *Geology* 27:171–174
- Filippelli GM, Carnahan JW, Derry LA, Kurtz A (2000) Terrestrial paleorecords of Ge/Si cycling derived from lake diatoms. *Chem Geol* 168:9–26
- French JJ, Busby MW (1974) Flood-hazard study—100-year flood stage for Baldwin Lake, San Bernardino County, California. U.S. Geological Survey Water-Resources Investigations
- Fridell JET, Guilderson TP, Kashgarian M (2003) Increased northeast Pacific climate variability during the warm middle Holocene. *Geophys Res Lett* 30:14-1–14-4
- Gale SJ, Hoare PG (1991) Quaternary sediments: a laboratory manual of the petrography of unlithified rocks. Belhaven Press, New York
- Geiss CE, Umbanhowar JCE, Banerjee SK, Camill P (2004) Sediment-magnetic signature of land-use and drought as recorded in lake sediment from south-central Minnesota, USA. *Quat Res* 62:117–125
- Gervais BR (2006) A three-century record of precipitation and blue oak recruitment from the Tehachapi Mountains, Southern California, USA. *Dendrochronologia* 24:29–37
- Grenda D (1997) Continuity and change: 8,500 years of lacustrine adaptation on the shores of Lake Elsinore. Statistical Research Technical Series, Redlands
- Gunatilaka A (1991) Palaeolimnology of Neusiedlersee, Austria. *Hydrobiologia* 214:239–244
- Hamilton PB, Gajewski K, Atkinson DE, Lean DRS (2001) Physical and chemical limnology of 204 lakes from the Canadian Arctic Archipelago. *Hydrobiologia* 457:133–148
- Hardie LA, Smoot JP, Eugster HP (1978) Saline lakes and their deposits: a sedimentological approach. In: Matter A, Tucker ME (eds) Modern and Ancient Lake sediments. Blackwell Scientific Publications, Oxford, 290 pp
- Harrison SP, Kutzbach JE, Liu Z, Bartlein PJ, Otto-Bliesner B, Muhs D, Prentice IC, Thompson RS (2003) Mid-Holocene climates of the Americas: a dynamical response to changed seasonality. *Clim Dyn* 20:663–688
- Heiri O, Lotter AF, Lemcke G (2001) Loss on ignition as a method for estimating organic and carbonate content in sediments: reproducibility and comparability of results. *J Paleolimnol* 25:101–110
- Heusser L (1978) Pollen in Santa Barbara Basin, California; a 12,000-yr record. *Geol Soc Am Bull* 89:673–678
- Hilton J, Lishman JP (1985) The effect of redox changes on the magnetic susceptibility of sediments from a seasonally anoxic lake. *Limnol Oceanogr* 30:907–909
- Hodell DA, Schelske CL, Fahnenstiel GL, Robbins LL (1998) Biologically induced calcite and its isotopic composition in Lake Ontario. *Limnol Oceanogr* 43:187–199
- Hovorka SD (1997) Quaternary evolution of ephemeral playa lakes on the Southern High Plains of Texas, USA: cyclic variation in lake level recorded in sediments. *J Paleolimnol* 17:131–146
- Hudson T (1978) Lake Elsinore Valley: its story. Mayhall Print Shop, Lake Elsinore
- Hull AG (1990) Seismotectonics of the Elsinore-Temecula trough, Elsinore fault zone, Southern California. Ph.D. Dissertation, University of California, Santa Barbara, 233 pp
- Inman DL, Jenkins SA (1999) Climate change and the episodicity of sediment flux of small California Rivers. *J Geol* 107:251–270
- Intergovernmental Panel on Climate Change (2001) Climate Change 2001: synthesis Report (<http://www.ipcc.ch/>)
- Jenkins PA, Duck RW, Rowan JS, Walden J (2002) Fingerprinting of bed sediment in the Tay Estuary, Scotland: an environmental magnetism approach. *Hydro Earth Syst Sci* 6:1007–1016
- Johnson TC, Brown ET, McManus J, Barry S, Barker P, Gasse F (2002) A high-resolution paleoclimate record spanning the past 25,000 years in Southern East Africa. *Science* 296:113–132
- Kelts K, Talbot MR (1990) Lacustrine carbonates as geochemical archives of environmental change and biotic/abiotic interactions. In: Tilzer MM, Serruya C (eds) Large Lakes: ecological structure and function. Springer-Verlag, New York, pp 288–315
- Kennett DJ (2005) The Island Chumash: behavioral ecology of a maritime society. University of California Press, Berkeley

- Kirby ME, Lund SP, Poulsen CJ (2005) Hydrologic variability and the onset of modern El Niño–Southern Oscillation: a 19 250-year record from Lake Elsinore, Southern California. *J Quat Sci* 20:239–254
- Kirby ME, Mullins HT, Patterson WP, Burnett AW (2002a) Late glacial–Holocene atmospheric circulation and precipitation in the northeast United States inferred from modern calibrated stable oxygen and carbon isotopes. *Bull Geol Soc Am* 114:1326–1340
- Kirby ME, Patterson WP, Mullins HT, Burnett AW (2002b) Post-younger Dryas climate interval linked to circumpolar vortex variability: isotopic evidence from Fayetteville Green Lake, New York. *Clim Dyn* 19:321–330
- Kirby ME, Poulsen CJ, Lund SP, Patterson WP, Reidy L, Hammond DE (2004) Late Holocene lake-level dynamics inferred from magnetic susceptibility and stable oxygen isotope data: Lake Elsinore, Southern California (USA). *J Paleolimnol* 31:275–293
- Kirby ME, Lund SP, Bird BW (2006) Mid-Wisconsin sediment record from Baldwin Lake Reveals Hemispheric Climate Dynamics (Southern CA, USA). *Palaeogeogr Palaeoclimatol Palaeoecol* 241:267–283
- Kutzbach JE (1981) Monsoon climate of the early Holocene: climate experiment with the earth's orbital parameters for 9000 years ago. *Science* 214:59–61
- Kutzbach JE, Guetter PJ (1986) The influence of changing orbital parameters and surface boundary conditions on climate simulations for the past 18 000 years. *J Atmos Sci* 43:1726–1759
- Kutzbach JE, Gallimore RG (1988) Sensitivity of a coupled atmosphere/mixed layer ocean model to changes in orbital forcing at 9000 years BP. *J Geophys Res* 93:803–821
- Last WM, Vance RE (1997) Bedding characteristics of Holocene sediments from salt lakes of the northern Great Plains, Western Canada. *J Paleolimnol* 17:297–318
- Latif M, Barnett TP (1994) Causes of decadal climate variability over the North Pacific and North America. *Science* 266:634–637
- Lau N-C (1988) Variability of the observed midlatitude storm tracks in relation to low-frequency changes in the circulation pattern. *J Atmos Sci* 45:2718–2743
- Lindstrom S (1990) Submerged tree stumps as indicators of mid-Holocene aridity in the Lake Tahoe Basin. *J Calif Gre Bas Anthro* 12:146–157
- Liu Z, Shields C, Otto-Bliesner B, Kutzbach J, Li L (2003) Coupled climate simulation of the evolution of global monsoons in the Holocene. *J Clim* 16:2472–2490
- Lorenz SJ, Kim JH, Rambu N, Schneider RR, Lohmann G (2006) Orbitally driven insolation forcing on Holocene climate trends: evidence from alkenone data and climate modeling. *Paleoceanography* 21:PA1002
- Lynch HB (1931) Rainfall and stream run-off in Southern California since 1769. Final report to the Metropolitan Water District of Southern California, Los Angeles, 31 pp
- Mann JF (1956) The origin of Elsinore Lake Basin. *Bull So Cal Acad Sci* 55:72–78
- Mann JF (1947) The sediments of Lake Elsinore. MSc Thesis, University of Southern California, 33 pp
- Mantua NJ, Hare SR (2002) The Pacific Decadal Oscillation. *J Oceanogr* 58:35–44
- McFadden MA, Patterson WP, Mullins HT, Anderson WT (2005) Multi-proxy approach to long- and short-term Holocene climate-change: evidence from eastern Lake Ontario. *J Paleolimnol* 33:371–391
- McGuire JC, Acton GD (2003) Composite depth scales for the Japan Trench, ODP LEG 186 Sites 1150 and 1151
- Meko DMS, Boggess WR (1980) A tree-ring reconstruction of drought in Southern California. *Water Resour Bull* 16:594–600
- Meyers PA, Ishiwatari R (1993) Lacustrine organic geochemistry—an overview of indicators of organic matter sources and diagenesis in lake sediments. *Org Geochem* 20:867–900
- Miller NLB, Strem E (2003) Potential impacts of climate change on California Hydrology. *J Am Water Resour Bull* 39:771–784
- Mitchell DL, Redmond K, Ivanova D, Rabin R, Brown TJ (2002) Gulf of California sea surface temperatures and the North American Monsoon: mechanistic implications from observations. *J Clim* 15:2261–2281
- Mullins HT (1998) Holocene lake level and climate change inferred from marl stratigraphy of the Cayuga Lake Basin, New York. *J Sed Res* 68:569–578
- Namias J, Cayan DR (1981) Large-scale air–sea interactions and short-period climatic fluctuations. *Science* 214:869–876
- Negrini RM (2002) Pluvial lake sizes in the Northwestern Great Basin throughout the Quaternary Period. In: Hershler R, Currey D, Madsen D (eds) Great Basin aquatics systems history. Smithsonian Press, Washington, 405 pp
- Negrini RM, Roberts AP, Cohen AS, Wigand PE, Foit FFJ, Erbes DB, Faber K, Herrera AM (2000) A paleoclimate record for the past 250,000 years from Summer Lake, Oregon, USA: I. Chronology and magnetic proxies for lake level. *J Paleolimnol* 24:125–149
- Negrini RM, Wigand PE, Draucker S, Gobalet K, Gardner JK, Sutton MQ, Yohe Li RM (2006) The Rambla high stand shoreline and the Holocene lake-level history of Tulare Lake, California, USA. *Quat Sci Rev* 25:1599–1618
- Owen LA, Finkel RC, Minnich RA, Perez AE (2003) Extreme southwestern margin of late Quaternary glaciation in North America: timing and controls. *Geology* 31:729–732
- Peck JA, King JW, Overpeck JT, Scholz CA, Green RR, Shanahan T (2004) A magnetic mineral record of Late Quaternary tropical climate variability from Lake Bosumtwi, Ghana. *Palaeogeogr Palaeoclimatol Palaeoecol* 215:37–57
- Pisias NG (1978) Paleoceanography of the Santa Barbara Basin and the California Current during the last 8000 years. *Quat Res* 10:366–384
- Plummer PS, Gostin VA (1981) Shrinkage cracks: desiccation or synaeresis? *J Sed Pet* 51:1147–1156

- Pyke CB (1972) Some meteorological aspects of the seasonal distribution of precipitation in the western United States and Baja California. University of California Water Resources Center, Los Angeles, 205 pp
- Redmond KT, Koch RW (1991) Surface climate and streamflow variability in the Western United States and their relationship to large-scale circulation indices. *Water Resour Res* 27:2381–2399
- Rees AWG, Hinton GCF, Johnson FG, O'Sullivan PE (1991) The sediment column as a record of trophic status: examples from Bosherton Lakes, SW Wales. *Hydrobiologia* 214:171–180
- Reheis MC, Kihl R (1995) Dust deposition in southern Nevada and California, 1984–1989: relations to climate, source area, and source lithology. *J Geophys Res* 100:8893–8918
- Reynolds RL, Callender E, Goldin A, Rosenbaum JG, Van Metre P, Tuttle M (1999) Greigite (Fe₃S₄) as an indicator of drought—the 1912–1994 sediment magnetic record from White Rock Lake, Dallas, Texas, USA. *J Paleolimnol* 21:193–206
- Reynolds RL, King JW (1995) Magnetic records of climate change. *Rev Geophys*:101–110
- Rosen MR (1991) Sedimentologic and geochemical constraints on the evolution of Bristol Dry Lake basin, California, USA. *Palaeogeogr Palaeoclimatol Palaeoecol* 84:229–257
- Rosenmeier MF, Hodell DA, Brenner M, Curtis JH, Martin JB, Anselmetti FS, Ariztegui D, Guilderson TP (2002) Influence of vegetation change on watershed hydrology: implications for paleoclimatic interpretation of lacustrine δ18O records. *J Paleolimnol* 27:117–131
- Rowntree LB (1985) A crop-based rainfall chronology for pre-instrumental record Southern California. *Clim Chan* 7:327–341
- Sawada M, Viau AE, Vettoretti G, Peltier WR, Gajewski K (2004) Comparison of North-American pollen-based temperature and global lake-status with CCCma AGCM2 output at 6 ka. *Quat Sci Rev* 23:225–244
- Schonher T, Nicholson SE (1989) The relationship between California rainfall and ENSO events. *J Clim* 2:1258–1269
- Seltzer GO, Tapia PM, Rowe HD, Dunbar RB, Rodbell DT, Baker PA, Fritz SC (2002) Early warming of tropical South America at the last glacial–interglacial transition. *Science* 296:1685–1686
- Smoot JP (1991) Sedimentary facies and depositional environments of early Mesozoic Newark Supergroup basins, eastern North America. *Palaeogeogr Palaeoclimatol Palaeoecol* 84:369–423
- Smoot JP, Benson LV (1998) Sedimentary structures as indicators of paleoclimatic fluctuations: Pyramid Lake, Nevada. In: Pitman J, Carroll A (eds) *Modern and Ancient Lakes: new problems and perspectives*. Utah Geological Association, Salt Lake City, 328 pp
- Smoot JP, Benson LV (2004) Mechanical mixing of climate proxies by sediment focusing in Pyramid Lake, Nevada: a cautionary tale. *Geological Society of America Abstracts with Programs*, 473 pp
- Spaulding WG (1990) Vegetational and climatic development of the Mojave Desert: the last glacial maximum to the present. In: Betancourt JL, Van Devender TR, Martin PS (eds) *Packrat middens: the last 40,000 years of biotic change*. The University of Arizona Press, Tucson, 469 pp
- Stuiver M, Reimer PJ, Bard E, Beck JW, Burr GS, Hughen KA, Kromer B, McCormac FG, Plicht J, Spurk M (1998) INTCAL98 radiocarbon age calibration, 24,000–0 cal BP. *Radiocarbon* 40:1041–1083
- Tang M, Reiter ER (1984) Plateau Monsoons of the Northern Hemisphere: a comparison between North America and Tibet. *Mon Wea Rev* 112:617–637
- Tarduno JA (1995) Superparamagnetism and reduction diagenesis in pelagic sediments: enhancement or depletion? *Geophys Res Lett* 22:1337–1340
- Teranes JL, McKenzie JA (2001) Lacustrine oxygen isotope record of 20th-century climate change in central Europe: evaluation of climatic controls on oxygen isotopes in precipitation. *J Paleolimnol* 26:131–146
- Thompson R, Battarbee RW, O'Sullivan PE, Oldfield F (1975) Magnetic susceptibility of lake sediments. *Limnol Oceanogr* 20:687–698
- Thompson JB, Schultze-Lam S, Beveridge TJ, Des Marais DJ (1997) Whiting events: biogenic origin due to the photosynthetic activity of cyanobacterial picoplankton. *Limnol Oceanogr* 42:133–141
- Trenberth KB, Hurrell JW (1994) Decadal atmosphere-ocean variations in the Pacific. *Clim Dyn* 9:303–319
- Tubbs AM (1972) Summer thunderstorms over Southern California. *Mon Wea Rev* 100:799–807
- USGS (1998) National water-quality assessment program—Santa Ana Basin
- Vaalgamaa S (2004) The effect of urbanisation on Laajalahti Bay, Helsinki City, as reflected by sediment geochemistry. *Mar Pollut Bull* 48:650–662
- Wells SG, Brown JB, Enzel Y, Anderson RY, McFadden LD (2003) Late Quaternary geology and paleohydrology of pluvial Lake Mojave, Southern California. In: Enzel Y, Wells SG, Lancaster N (eds) *Paleoenvironments and paleohydrology of the Mojave and Southern Great Basin Deserts*. Geological Society of America, Boulder, 260 pp
- Wilkinson RC, Goodchild M, Reichman J, Dozier J (2002) The potential consequences of climate variability and change: The California Regional Assessment. A Report of the California Regional Assessment Group for the U.S. Global Change Research Program, 432 pp (http://www.ncgia.ucsb.edu/pubs/CA_Report.pdf)
- Willemsse NW, Tornqvist TE (1999) Holocene century-scale temperature variability from West Greenland lake records. *Geology* 27:580–584
- Williams J (2005) Background: California's tropical storms. *USA Today*. Los Angeles
- Wohlfahrt J, Harrison SP, Braconnot P (2004) Synergistic feedbacks between ocean and vegetation on mid- and high-latitude climates during the mid-Holocene. *Clim Dyn* 22:223–238